

RESEARCH

Open Access



Ecotoxicological assessment of cigarette butts on morphology and photosynthetic potential of *Azolla pinnata*

Garishma Shah¹, Upma Bhatt¹, Hanwant Singh¹, Deepak Kumar¹, Jyotshana Sharma¹, Reto J Strasser² and Vineet Soni^{1*}

Abstract

Cigarette butts (CBs) have become the most ubiquitous form of anthropogenic litter globally. CBs contain various hazardous chemicals that persist in the environment for longer period. These substances are susceptible to leaching into the environment through waterways. The recent study was aimed to evaluate the effects of disposed CBs on the growth and development of *Azolla pinnata*, an aquatic plant. It was found that after a span of 6 days, the root length, surface area, number of fronds, and photosynthetic efficacy of plant were considerably diminished on the exposure of CBs (concentrations 0 to 40). The exposure of CBs led to a decrease in the F_{Mv} , F_v/F_o , and ϕP_o , in contrast, the ϕD_o increased in response to CBs concentration. Moreover, ABS/CSm , TR_o/CSm , and ET_o/CSm displayed a negative correlation with CB-induced chemical stress. The performance indices were also decreased (p -value ≤ 0.05) at the highest concentration of CBs. LD_{50} and LD_{90} represent the lethal dose, obtained value for LD_{50} is 20.30 CBs and LD_{90} is 35.26 CBs through probit analysis. Our results demonstrate that the CBs cause irreversible damage of photosynthetic machinery in plants and also reflect the efficacy of chlorophyll *a* fluorescence analysis and JIP test for assessing the toxicity of CBs in plants.

Keywords Cigarette butts, Chlorophyll fluorescence, Energy fluxes, Quantum yield, Performance index, Photosynthesis

Introduction

Cigarette butts (CBs) have unfortunately maintained their position as the most prevalent form of litter item globally since the 1990s [1–3]. Approximately, 4.5 trillion CBs are discarded into the atmosphere each year [2] and in which 76 % to 84 % of smokers discard their CBs directly on the land instead of disposing them in a bin [4,

5]. This contribute 22–46 % visible waste in metropolitan areas worldwide [4–6]. An average density of finding CBs in an area is 2.7 CBs m^{-2} highest is 47 CBs m^{-2} in Berlin [7]. Most of CBs consist with a filter to ease the direct effect of CBs chemicals to smokers. This filter is fabricate by 12,000 cellulose acetate fibers and can persist in the surroundings for an unknown period [8, 9]. When discarded, CBs often contain un-smoked tobacco and various toxicants like nicotine, polycyclic aromatic hydrocarbons (PAHs) [7], formaldehyde, BTEX [10], acrolein, benzene derivatives, polycyclic aromatic amines [11, 12], poisonous gases, tar, and heavy metals, [13]. Some cigarettes also contain flavorings agents mostly in menthol based cigarettes, such as 5-methyl-2-(propan-2-yl)cyclohexan-1-ol [14, 15]. Improper disposal of CBs

*Correspondence:

Vineet Soni
vineetpbb1154@gmail.com

¹ Plant Bioenergetics and Biochemistry Lab, Mohanlal Sukhadia University, Udaipur, Rajasthan, India 313001

² Plant Bioenergetics Laboratory, University of Geneva, Jussy, 1254 Geneva, Switzerland



© The Author(s) 2024. **Open Access** This article is licensed under a Creative Commons Attribution 4.0 International License, which permits use, sharing, adaptation, distribution and reproduction in any medium or format, as long as you give appropriate credit to the original author(s) and the source, provide a link to the Creative Commons licence, and indicate if changes were made. The images or other third party material in this article are included in the article's Creative Commons licence, unless indicated otherwise in a credit line to the material. If material is not included in the article's Creative Commons licence and your intended use is not permitted by statutory regulation or exceeds the permitted use, you will need to obtain permission directly from the copyright holder. To view a copy of this licence, visit <http://creativecommons.org/licenses/by/4.0/>. The Creative Commons Public Domain Dedication waiver (<http://creativecommons.org/publicdomain/zero/1.0/>) applies to the data made available in this article, unless otherwise stated in a credit line to the data.

on land leads to the toxicants becoming accessible in plants and animals [16, 17]. This is due to the chemicals being easily washed into the environment through waterways and runoff when exposed to atmospheric moisture and rain [7, 18] . . The detrimental effects of cigarettes on human health are widely documented in the literatures [15]. Still, there is a lack of understanding about their environmental impacts.

In aquatic habitats, these toxic compounds can leach, causing harm to marine and fresh water organisms. Evidence suggests that aquatic organisms, such as *Ceriodaphnia dubia* [18], *Pimephales promelas* [13], bacteria, *Hediste diversicolor* [19], gastropods [20], and *Atherinops affinis* [13], are vulnerable to the lethal properties of these compounds. Interestingly, even un-smoked CBs were found to be lethal to freshwater fishes and few marine fishes, also in the some species of fresh water fishes have unconscious nervous system on the exposure of high CBs concentration [13]. The accessibility of toxic substances to organisms is influenced by their leaching capacity [21]. Nicotine, for instance, is highly soluble in water, especially under alkaline conditions, and can percolate from CBs over time [22]. Several plant products, including food crops, teas, and spices, have been found to contain nicotine, which can be taken up by plants from tobacco smoke or soil littered with commercial tobacco [22]. Recent short-term experimental exposure to leachate from smoked cigarette filters showed mutagenic, genotoxic, and cytotoxic effect in onion plants [23]. However, the effects of littered CBs on plant germination, growth, and chlorophyll amount, photosynthesis are not well understood [24].

Azolla (Lam.), commonly mosquito fern, is a fast-growing, free-floating aquatic plant that has been widely used in aquatic biology research due to its rapid growth.

This plant has numerous applications, including its use as a livestock feed, human food, bio-fertilizer, and a bio-fuel [25]. Among the diverse species of mosquito fern, *Azolla pinnata* has been one of the most frequently used in experimental works because of its large abundance in rice fields, reservoirs and polluted ponds. Several studies found to assess toxicity of Pb [26], Cd, Cr [27], rhodamine B dye [28] using *A. pinnata* plant. Our study focused to assess the impact of CBs exposure on the physiology and morphology of *A. pinnata*, with a particular emphasis on photosynthetic efficiency using various parameters. Chlorophyll *a* fluorescence (ChlF) is a widely used non-persisting technique to sense plant stress conditions, and it is often combined with other physiological and chemical variables [29, 30]. ChlF describes the natural procedure by which absorbed energy is not utilized for photosynthesis which is dissipated as heat or re-emitted, providing a quantitative assessment of oxygenic photosynthesis [31]. CBs exposure disrupts photosynthesis by chemically interacting with proteins and increasing reactive oxygen species generation [32, 33]. This study provide a wide information about the impact of CBs on plants only some basics elementary studies has been done and mentioned in the Table 1 [34]. The study provides the impact of severity of CBs on plants growth, metabolism and physiology. The hypothesis that on the continuous and long exposure of CBs in the atmosphere produces ill effect in plant measure with the help of physiological and morphological observation.

Materials and methods

Plant material and CBs collection

Azolla pinnata plants were obtained from a pond located at the botanical garden of the Department of Botany, Mohanlal Sukhadia University, Udaipur, India

Table 1 Previous elementary work on exposure of CBs on different plants

S.N.	Plant species	Effect of Chemical released by Cigarette Butts	
1	<i>Glycine max</i>	Reduction in vessels diameter, ylem and phloem in vascular bundles	(Weryszko-Chmielewska & Chwil, 2005)
2	<i>Pisum sativum</i>	Reduction observed in biomass, root/shoot ratio and leaf area	(Çimrin et al., 2007)
3	<i>Cicer arietinum</i>	Reduction in number of leaves	(Das et al., 2012)
4	<i>Arabidopsis thaliana</i>	Reduction in lipid peroxidation, reactive oxygen species, GSH and ascorbate which lead to cell death	(Zhao & Yi, 2014)
5	<i>Lolium perenne</i>	Initial growth being stunted	(Green et al., 2019) [35]
6	<i>Brassicca napus</i>	Reduce root length due to the exposure of PAHs	(Zhao & Yi, 2014)
7	<i>Gossypium hirsutum</i> and <i>Catharanthus roseus</i>	Low photo synthesis due to reduction in chlorophyll a and b and plant is in stress	(Iori et al., 2017)
8	<i>Triticum aestivum</i>	Seedling shows genotoxic effect, growth retardation and cellular damage observed	(Abbas et al., 2017)
9	<i>Allium cepa</i>	Cytotoxic, genotoxic and mutagenic effect	(Montalvão et al., 2019) [23]
10	<i>Suaeda salsa</i>	High concentration produce adverse effect on the growth	(Xu et al., 2020)

(coordinates 24° 34'54" N and 73° 42'40" E). The plant specimen was identified by Dr. Vineet Soni on the basis of characteristic like leaves are tiny, lacy-looking, and closely overlapping, leaves can be green or rusty red and short, branched, floating stem, bearing roots which hang down in the water. The leaves are alternately arranged, each consisting of a thick aerial dorsal lobe containing green chlorophyll and a slightly larger thin, colourless, floating ventral lobe and deposited in the herbarium of the Department of Botany, MLS University, Udaipur, India, with accession number-MLSU/BOT/00227896. CBs were collected randomly from roadsides, parks, and smoking areas. The collected CBs were of similar length but from different brands. For the experiment, surrounding trapping paper of CBs was removed by the help of forceps and scissors. The CBs were dried overnight at 40 °C and then used to prepare concentrated leachate of different concentrations 10CBs L⁻¹, 20 CBs L⁻¹, 30 CBs L⁻¹, 40 CBs L⁻¹ [36]. The experiment was repeated several time in order to screen the concentration of CBs. On the basis of these primary screenings, the best and suitable concentration of CBs in number per liter was selected for further studies. The leachate samples were subjected to an ecotoxicological test to assess their potential environmental impact.

Experimental design

After being collected, *A. pinnata* plants were transferred to a water tank amended with a solution called MPK solution 1 g L⁻¹ (Magnesium chloride, rock phosphate, and potassium salt in 1:2:1 w/w/w ratio) every 15 days for propagation at the Plant Bioenergetic and Biochemistry Laboratory at MLS University in Udaipur, India. For the experiments, healthy 7-day-old plants were moved into 1 L glass containers filled with a nutrient solution containing 1000 μM (NH₄)₂SO₄, 1000 μM Ca(NO₃)₂, 500 μM K₂SO₄, 500 μM MgSO₄, 250 μM KH₂PO₄, 10 μM Fe-EDTA, 10 μM H₃BO₃, 0.5 μM MnCl₂, 0.5 μM ZnSO₄, 0.1 μM CuSO₄, and 0.1 μM (NH₄)₆Mo₇O₂₄ (pH of the nutrient solution was adjusted to 6.5 ± 0.2 applying NaOH or H₂SO₄) and placed in the plant growth chamber. All chemicals are purchased from Sigma-Aldrich, Udaipur, India. The chamber was maintained at specific environmental conditions including a 16-hour light and 8-hour dark photoperiod with an intensity of 50 μmol photons m⁻² s⁻¹, temperature is 25–28 °C, and 70–75 % relative humidity. After one week acclimatization period, plants (≈ 50 healthy fronds) were relocated to 1 L glass containers (having 20 cm diameter and 10 cm height) with diverse concentrations of CBs (10, 20, 30, 40 CBs) mixed with the same nutrient solution and allowed to grow for 6 days. Each treatment had three independent replicates (N=3) and an equal amount of plant biomass.

Measurement of morphological parameters

Determination of Average Fronds area (AFA), Average fronds number (AFN) and Average root length (ARL), specific morphological variability in *A. pinnata* exposed to CBs, the Fiji-Image J software (an open-source software used for advanced processing and scientific analyses of images, [https:// imagej.net/Fiji](https://imagej.net/Fiji)) was used. Plant images were captured every interval of 3 days for up to 6 days duration using a DSLR camera (Nikon D7500, Resolution 20.9MP and distance from object is 70 cm) under dispersed light conditions.

Measurement of chlorophyll a fluorescence

The plant efficiency analyzer Handy PEA fluorimeter, manufactured by Hansatech Instruments Ltd. England, was used to measure ChlF. Prior to measurement; fronds were subjected to a dark adaptation period of 50–60 minutes at 26 °C. The Biolyzer v.3.0.6 software, developed by the Laboratory of Bioenergetics at the University of Geneva, Switzerland, was used to analyze the ChlF signals. To ensure the accuracy of the results, the experiments were performed in six replicates and repeated thrice times. The JIP-test method was utilized to calculate various phenomenological and biophysical parameters that quantify the behaviors of both the photosystem I (PSI) and photosystem II (PSII). The polyphasic ChlF rise, also known as the OJIP curve, provided valuable information about photosynthetic fluxes, and numerous parameters were derived from it [37, 38] \ Table 2 presents the definitions, formulas, and abbreviations for the JIP-test parameters utilized in the current study.

Statistical analysis

In this study, a statistical analysis was performed to evaluate the significance of measurements using ANOVA conducted by a Tukey HSD test ($p = 0.05$) with the use of SPSS software (version 22.0). The figures presented only include measurements that had a significant value of $p \leq 0.05$. To create an unbiased color code, the values were normalized and scaled between 1 and 100, with a color scheme of red indicating high values (100%), yellow indicating medium values (50%), and green indicating low values (1%) used to generate the heat map. The correlation grid was designed using Microsoft Excel and Canva software. Additionally, a principal component analysis (PCA) was performed using Origin Pro 2018 software to identify any patterns and variations in the experimental data through eigenvalue decomposition of a data correlation matrix. The ChlF parameter was selected for the PCA analysis, which helped in identifying the variables that showed the highest fluctuations. The results showed that dimension 2 (PC 2) accounted for 74.09

Table 2 The JIP-test parameters, along with their respective abbreviations, formulas, and definitions, are presented

BASIC PARAMETERS CALCULATED FROM THE EXTRACTED DATA

$$F_0 \cong F_{50\mu s} \text{ or } \cong F_{20\mu s}$$

$$t_{FM} = t_{F_{MAX}}, t \text{ for } F_M$$

$$FM (=FP)$$

$$FV \equiv FM - F_0$$

$$SM \equiv \text{Area}/(FM - F_0) = \text{Area}/FV$$

$$N = SM \times (MO/VJ)$$

$$V_j = (F_j - F_0)/(F_M - F_0)$$

$$V_i = (F_i - F_0)/(F_M - F_0)$$

BIOPHYSICAL PARAMETERS DERIVED FROM THE BASIC PARAMETERS

Deexcitation rate constant of PSII antenna

$$kN_{\text{ABS}} = kF \times (1/FM)$$

$$kP_{\text{ABS}} = kF \times (1/F_0 - 1/FM) = kN \times (FV/F_0)$$

Specific energy fluxes (per RC: QA-reducing PSII reaction centre), in ms^{-1}

$$ABS/RC_{\text{MO}} = MO \times (1/VJ) \times (1/\phi P_0)$$

$$TRO/RC_{\text{MO}} = MO \times (1/VJ)$$

$$ETO/RC_{\text{MO}} = MO \times (1/VJ) - (1-VJ)$$

$$DIO/RC_{\text{MO}} = ABS/RC - TRO/RC$$

Phenomenological energy fluxes (per CS: QA-reducing PSII cross section), in ms^{-1}

$$TRO / CS_{M=} (FV/F_M) (ABS/CS_M)$$

$$ETO / CS_{M=} (FV/F_M) (1 - V_j) (ABS/CS_M)$$

$$DIO / CS_{M=} (ABS/CSO) - (TRO/CS_M)$$

$$ABS / CS_{M=} \approx F_0$$

Quantum yields and efficiencies

$$\phi P_0 = TRO/ABS = [1 - (F_0/FM)]$$

$$\phi E_0 = ETO/ABS = [1 - (F_0/FM)] (1 - VJ)$$

$$\psi E_0 = ETO/TRO = (1 - VJ)$$

$$\phi D_0 = F_0/F_M$$

Performance indexes

$$PI_{ABS} = \frac{1 - (F_0/F_M)}{MO/V_j} \times \frac{F_M/F_0}{F_0} \times \frac{1 - V_j}{V_j}$$

$$PI_{CS} = \frac{ABS}{CS} \times \frac{1 - (F_0/F_M)}{MO/V_j} \times \frac{F_M/F_0}{F_0} \times \frac{1 - V_j}{V_j}$$

fluorescence when all PSII RCs are open (\cong to the minimal reliable recorded fluorescence) [39]

Time (in ms) to reach maximal fluorescence F_M [39]

maximal fluorescence, when all PSII RCs are closed (=FP when the actinic light intensity is above $500 \mu\text{mol} (\text{photon}) \text{m}^{-2} \text{s}^{-1}$ and provided that all RCs are active as QA-reducing) [39]

maximal variable fluorescence [39]

Normalised Area to F_M [39]

Turnover number (expresses how many times QA is reduced in the time interval from 0 to t_{F_M}) [39]

Relative variable fluorescence at $t = 2 \text{ ms}$ [39]

Relative variable fluorescence at $t = 30 \text{ ms}$ [39]

Nonphotochemical deexcitation rate constant (ABS: absorption flux - see below; kF: rate constant for fluorescence emission) [39]

Photochemical deexcitation rate constant [39]

Absorption flux (exciting PSII antenna Chl a molecules) per RC (also used as a unit-less measure of PSII apparent antenna size) [39]

Trapped energy flux (leading to Q_A reduction), per RC [39]

Electron transport flux (further than Q_A^-), per RC [39]

Dissipated energy flux per RC (at $t = 0$) [39]

Trapped energy flux (leading to Q_A reduction) per RC (Tsimilli-Michael, 2020 [39])

Electron transport flux (further than Q_A^-) per RC (Tsimilli-Michael, 2020 [39])

Total energy dissipated per reaction center (RC) (Tsimilli-Michael, 2020 [39])

Absorbed photon flux per excited PSII cross section at time zero [39]

Maximum quantum yield for primary photochemistry [39, 40]

Quantum yield for electron transport (ET) [41]

Efficiency/probability that an electron moves further than Q_A^- [41]

Quantum yield (at $t = 0$) of energy dissipation [41]

Performance index for energy conservation from photons absorbed by PSII until the reduction of intersystem electron acceptors [39, 41]

Performance index on cross section basis [39, 41]

% of the maximum variability, while dimension 1 (PC 1) accounted for 19.63 %. The correlation between the parameters was analyzed using a grid correlation matrix and expressed using a color code between +1 and -1 by using python software [42, 43]. Probit Analysis, with the use of SPSS (22.0), was conducted to determine the lethal dose (LD_{50} and LD_{90}), while a Chi-square test was employed to compare the mortality ratios between experimental and control groups at varying concentrations.

Results:

The growth and productivity of *A. pinnata* was significantly affected by the occurrence of CBs, which caused modulation of the plant's photosynthetic process. To investigate this phenomenon, the current study explored the impact of CBs on various parameters of *A. pinnata*, including morphological parameters, chlorophyll fluorescence, specific energy fluxes, phenomenological energy fluxes, and performance indexes.

Morphological parameters

The study observed a significant decrease in the average frond area (AFA) of *A. pinnata* with increasing concentrations of CBs, with a standard deviation of ± 0.1 . The reduction in AFA was found to be continuous as the concentration of CBs increased. By the 6th day of the experiment, the AFA was decreased by 3% compared to the control plants. Additionally, the root length (ARL) of *A. pinnata* was found to be reduced from 5–6 cm in control plants to 0.25 cm in plants exposed to CBs. Differential changes in AFA and ARL are present in Fig. 1 (A to E). The increase in CBs concentration was also found to have a negative impact on plant mortality, with a reduction in the number of fronds (AFN) observed. At the end of the experiment, average two plants were found to be alive in the 40 CBs concentration condition shown in Fig. 2. These findings suggest that exposure to CBs has a significant negative impact on the growth and survival of *A. pinnata*.

Biochemical parameters

Throughout the experiment the chl *a* and *b* concentration were significantly decrease with the increasing concentration of CBs. Highest value of chl *a* and *b* were observed in the control system is 0.625 ± 0.022 and 0.443 ± 0.026 , respectively. The lowest value is approximate half value from control as demonstrate in the Table 3.

Chlorophyll a fluorescence (ChlF) kinetics

ChlF of *A. pinnata* was measured after 24 h of CBs treatment and a typical OJIP induction curve was displayed when plotted on the logarithm time scale in Fig. 3D. With increasing the CBs concentration, the fluorescence

yield at various intermediary steps, such as J, I, and P was reduced. In control plants, two intermediate peaks F_J (chlorophyll fluorescence at 2 ms) and F_I (chlorophyll fluorescence at 300 ms) were formed between F_0 and F_M , ChlF increased continuously from F_0 to F_M fluorescence intensity in *A. pinnata* growing under control conditions. CBs induced reduction in PSII photochemistry and electron transport activity were severe at the highest concentration of CBs.

Biophysical parameters

The concentration of CBs has been found to decrease both the smallest fluorescence intensity (F_0) and the maximum fluorescence intensity (F_M), as shown in Figs. 3A & 4. F_0 represents the fluorescence intensity measured at $50 \mu\text{s}$ when the primary (1°) quinone acceptor (Q_A) is in the oxidized state. The effectiveness of photosynthesis in plants is closely related to the maximum 1° yield of photochemistry of PSII, which is reflected by the F_v/F_0 ratio supposed to be relation of the rates at which excited Chl pigment undergo photochemical and non-photochemical deactivation. Raising value of F_v/F_0 indicates proper performance of PSII. However, the F_v/F_0 ratio for *A. pinnata* plants decreased steadily with increasing CBs concentration, as shown in Figs. 3A & 4. At 10 CBs, the F_v/F_0 ratio was 79.13 % of control, while at 20 CBs; it decreased to 40.55 % of control. Similarly, at 30 CBs and 40 CBs, the F_v/F_0 ratio was found to be 41.73 % and 19.29 % of control, respectively.

V_j is the relative variable fluorescence at 2 ms (J step) which measures the 1° quinone e^- acceptor of PSII in its reduced state [Q_A^-/Q_A (total)] [41]. V_j was found to increase as the concentration of CBs amplified. The

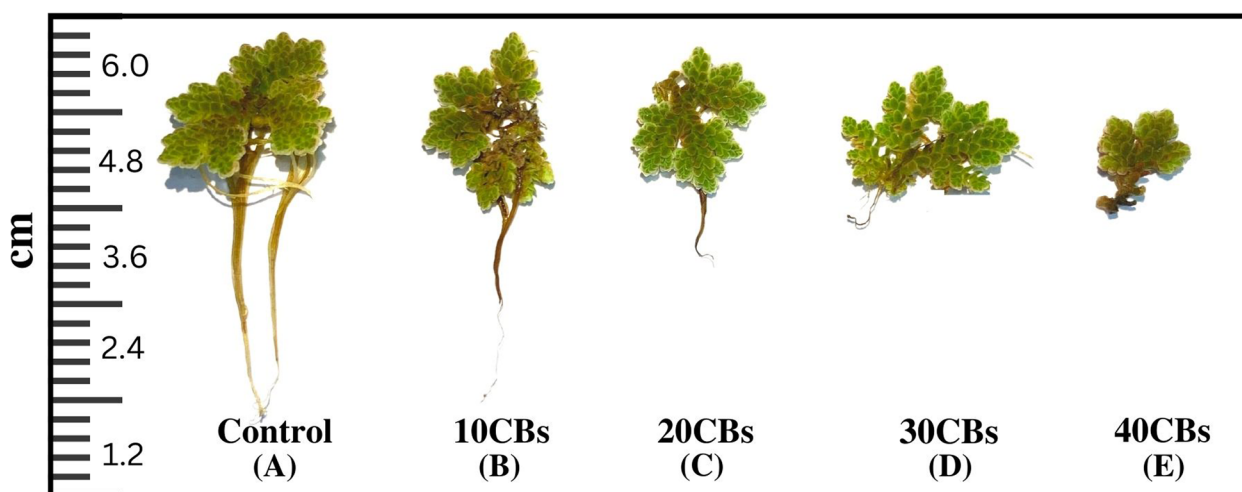


Fig. 1 Morphological changes in the *A. pinnata* during exposure of differential concentration of CBs (A) 0 CBs, (B) 10 CBs, (C) 20 CBs, (D) 30 CBs, (E) 40 CBs

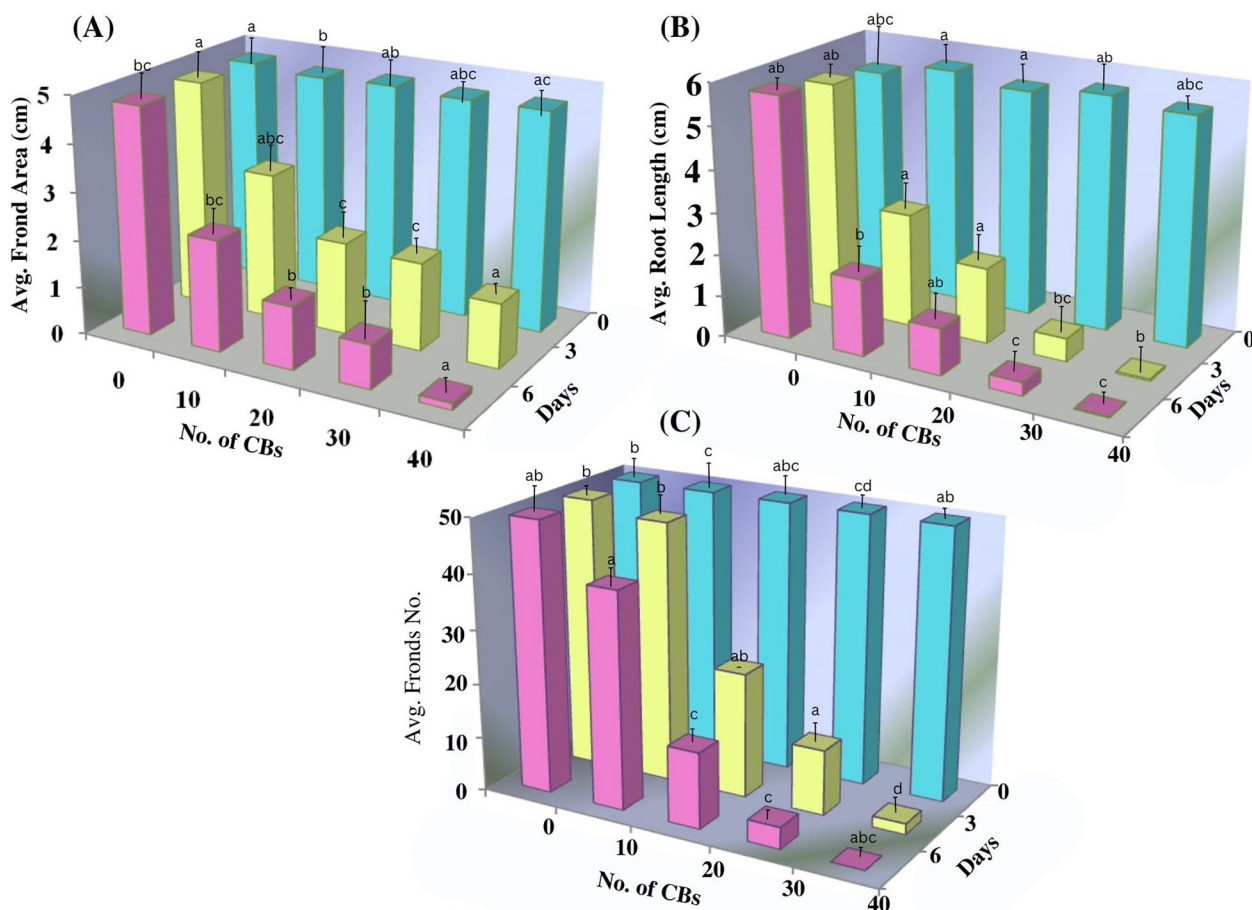


Fig. 2 3D bar graph representing the (A) change in average surface area (ASA), (B) change in average root length (ARL), (C) change in average fronds number (AFN) in *A. pinnata* on the exposure of differential concentration of CBs (0 to 40 CBs)

Table 3 Mean values of the Chlorophyll *a* and chlorophyll *b* content measured in *A. pinnata* after exposure of various concentrations of CBs

S.No.	Treatment	Chl <i>a</i> (mg g ⁻¹ FW)	Chl <i>b</i> (mg g ⁻¹ FW)
1.	Control	0.625 ± 0.022 ^a	0.443 ± 0.026 ^a
2.	10 CBs	0.557 ± 0.003 ^a	0.425 ± 0.002 ^a
3.	20 CBs	0.412 ± 0.018 ^b	0.339 ± 0.010 ^{ab}
4.	30 CBs	0.327 ± 0.041 ^b	0.311 ± 0.009 ^{bc}
5.	40 CBs	0.25 ± 0.038 ^c	0.205 ± 0.019 ^c

X ± *S* for three replicate measurements at a 95% level of confidence. Different letters indicate a significant difference (*P* ≤ 0.05)

maximum raise observed was up to 149 % of control value at 30 CBs, as depicted in Figs. 3A & 4.

The Complimentary Area (*S_M*) is a crucial factor that is directly linked to the number of redox events (reduction and oxidation) of one *Q_A* molecule throughout the rapid OJIP transient, in short the number of *e⁻* that pass through the electron transport chain (ETC) [40]. The

Turnover Number (*N*) refers to the number of times that *Q_A* is reduced and re-oxidized until *F_m* is attained [44–46]. In *A. pinnata*, both *S_M* and *N* values decrease with an increase in CBs concentration (Figs. 3A & 4). Specifically, *S_M* decreases by up to 8.7 % from the control, while *N* decreases by up to 7.1 % of control at the highest CBs concentration.

Quantum yield

The introduction of CBs in plants led to a slight reduction in the quantum yield of 1° photochemistry (*φP₀*) and electron transport (*φE₀*), which are indicators of the complete photosynthetic efficiency of active PSII reaction centre (RC). This trend was evident in both Figs. 3C and 4. The minimal values of *φP₀* and *φE₀*, which were approximately half of control, were recorded when *A. pinnata* was exposed to 40 CBs. In contrary, the quantum yield of dissipation (*φD₀*) showed a continuous enhancement with increasing CBs concentration, with approximately a two-fold increment observed from the control in the 40 CBs condition.

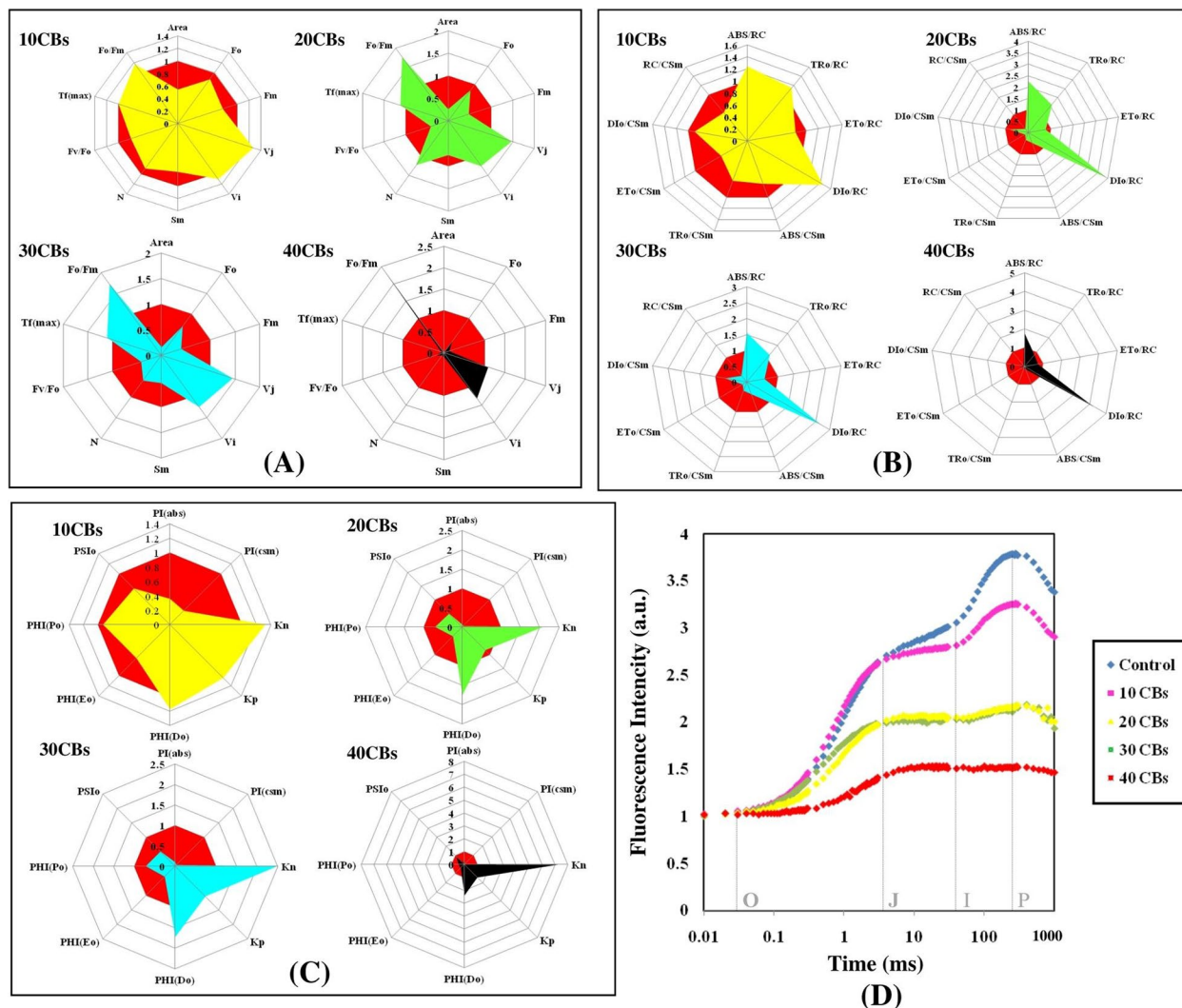


Fig. 3 The technical fluorescence parameters were represented by radar plots (A-C), with each line showing the average of 6 measurements per treatment and statistical significance was determined at $p \leq 0.05$ levels. Plot (D) The study measured ChlF in *A. pinnata* plants exposed to varying concentrations of CBs (0-40) for 24 hours, using PSII rapid fluorescence transients (O, J, I, and P) as indicators

Specific energy flux (membrane model)

The study analyzed the photosynthetic performance of active PSII RC of *A. pinnata* under differential concentrations of CBs by examining specific energy fluxes such as absorption energy (ABS/RC), trapped energy (TR₀/RC), electron transport (ET₀/RC), and dissipated energy (DI₀/RC) flux per reaction centre, showing in Figs. 3B & 5(II). The results showed a significant increase in ABS/RC and TR₀/RC at 40 CBs condition, indicating an enhancement in the absorption potential of active RC (Figs. 3B, 4). TR₀/RC was highly raised at 30 CBs condition that is 110.75 % of control. When exposed to increasing concentrations of CBs, the plants

showed a decrease in ET₀/RC, and at higher treated conditions, it reached 72.72 % of the control. On the other hand, the DI₀/RC displayed a significant increase in a sequential manner, with around a fivefold increment noted in plants treated with 40 CBs in comparison to the control. The study utilized thylakoid membrane models to diagrammatically present the effects of CBs on specific energy fluxes 5(II). Moreover, the study investigated whether CBs alters the ABS to active PSII RC ratio. The findings indicated that severe CBs stress results in more inactive RC and reduced ability of RC to reduce plastoquinone, as reflected by higher values of specific energy fluxes (ABS/RC, TR₀/RC, and DI₀/RC) in the leaf pipeline model.

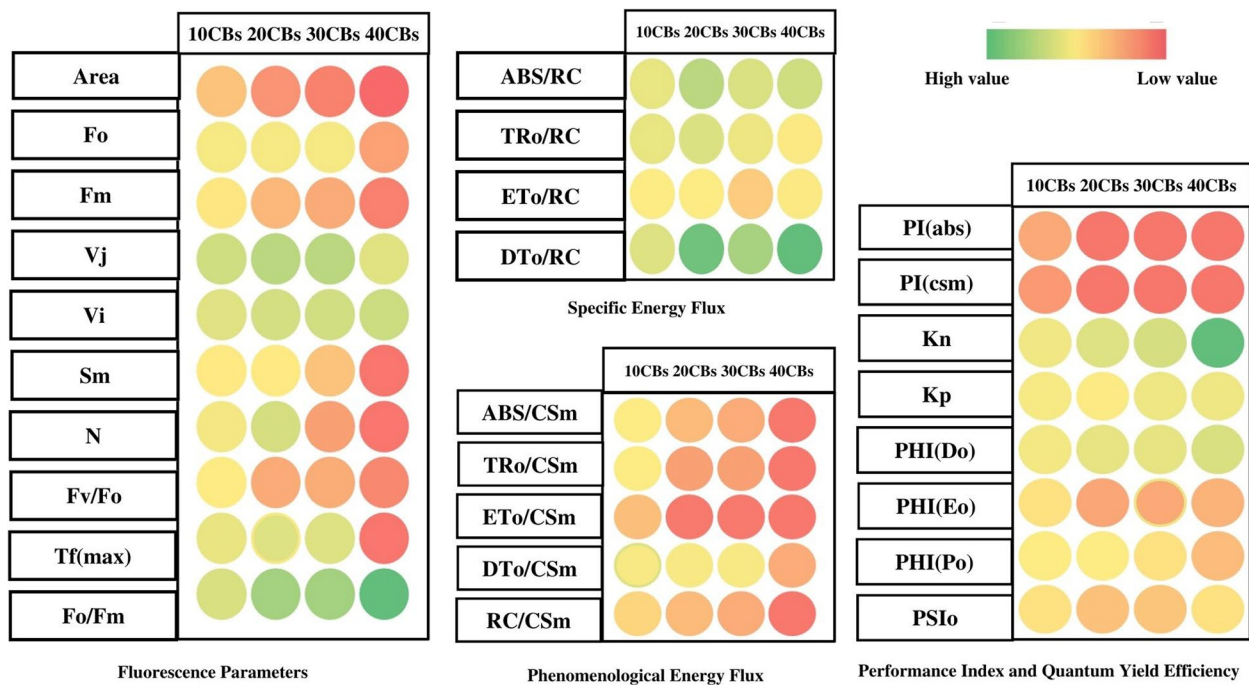


Fig. 4 A heat map was used to illustrate the relative variability of multiple photosynthesis-related parameters obtained from the JIP test on *A. pinnata* plants under CBs stress. The data was collected for varying concentrations (0-40) after 24 hours, with red indicating lower values (1%), yellow indicating medium (50%), and green indicating the highest values (100%). Prior to color coding, all data was normalized to maintain unbiased results within a range of 1-100 for the parameter values

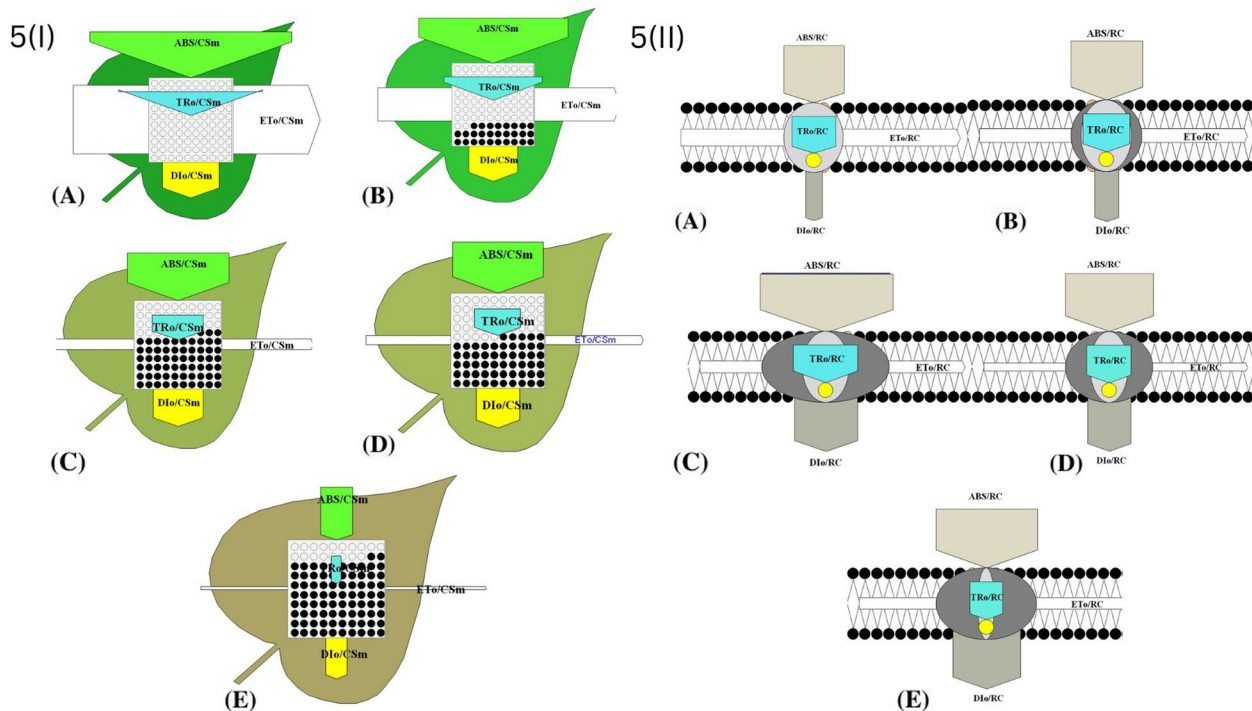


Fig. 5 (I): The study utilized an energy pipeline leaf model to investigate the phenomenological fluxes (per cross section, CS) in *A. pinnata* fronds under different concentrations of CBs, (A); control, (B); 10 CBs (C); 20 CBs (D); 30 CBs and (E); 40 CBs. (II): The study employed a thylakoid membrane model to analyze the specific energy fluxes (per reaction, RC) in *A. pinnata* fronds exposed to various concentrations of CBs, (A); control, (B); 10 CBs (C); 20 CBs (D); 30 CBs and (E); 40 CBs

Phenomenological energy flux (leaf model)

The impact of CBs-induced stress on *A. pinnata* was observed through changes in phenomenological energy fluxes such as absorption (ABS/C_{Sm}), trapped energy (TR/C_{Sm}), electron transport (ET/C_{Sm}), and dissipated energy (DI/C_{Sm}) flux per cross section. All these parameters showed significant reduction with increasing CBs concentration in *A. pinnata*. Specifically, at the 40 CBs condition, ABS/C_{Sm}, TR/C_{Sm}, ET/C_{Sm}, and DI/C_{Sm} decreased by 0.13 %, 6 %, 27.15 %, and 32.90 %, respectively, compared to the control Fig. 5 (I).

K_p and K_N

Under CBs stress, the rate constants for non-photochemical de-excitation reactions (K_N) were found to increase, and at severe stress levels, the K_N value reached up to 741.66 % of control, as depicted in Figs. 3C and 4. On the other hand, the de-excitation rate constants for photochemical reactions (K_p) only showed a slight increase under all stress conditions.

Performance Index

A radar plot (Figs. 3, 4) was used to illustrate the overall impact of CBs-induced stress on various photosynthetic parameters. In order to assess the effects of CBs on the overall performance of photosynthesis, PI_{ABS} (performance index on absorption basis) and PI_{CS} (performance index of PSII and PSI) were measured in *A. pinnata* plants subjected to different intensities of CBs stress. The results showed that CBs had a significant effect on PI_{ABS} and PI_{CS}, with both parameters decreasing continuously as the concentration of CBs increased. The lowest values of PI_{ABS} and PI_{CS} were recorded, which were respectively 11 times and 80 times lower than the control (as shown in Figs. 3C and 4). The results of the PCA analysis showed that the first two principal components, Dim 1 and Dim 2, explain 93.71% of the total variation in the ChlF parameter under CBs induced stress in *A. pinnata* (Fig. 6). The loadings for several JIP parameters are located in quadrant I and IV, including ET₀/RC, ET₀/C_{Sm}, PI_{CS}, PI_{ABS}, ABS/RC, TR₀/RC, and DT₀/RC. Meanwhile, TR₀/C_{Sm}, ABS/C_{Sm}, DI₀/C_{Sm}, F₀, F_M, and F_v/F₀ are accounted for in quadrant II. Most treatments, except for the 40 CBs treatment, are found in quadrant II and

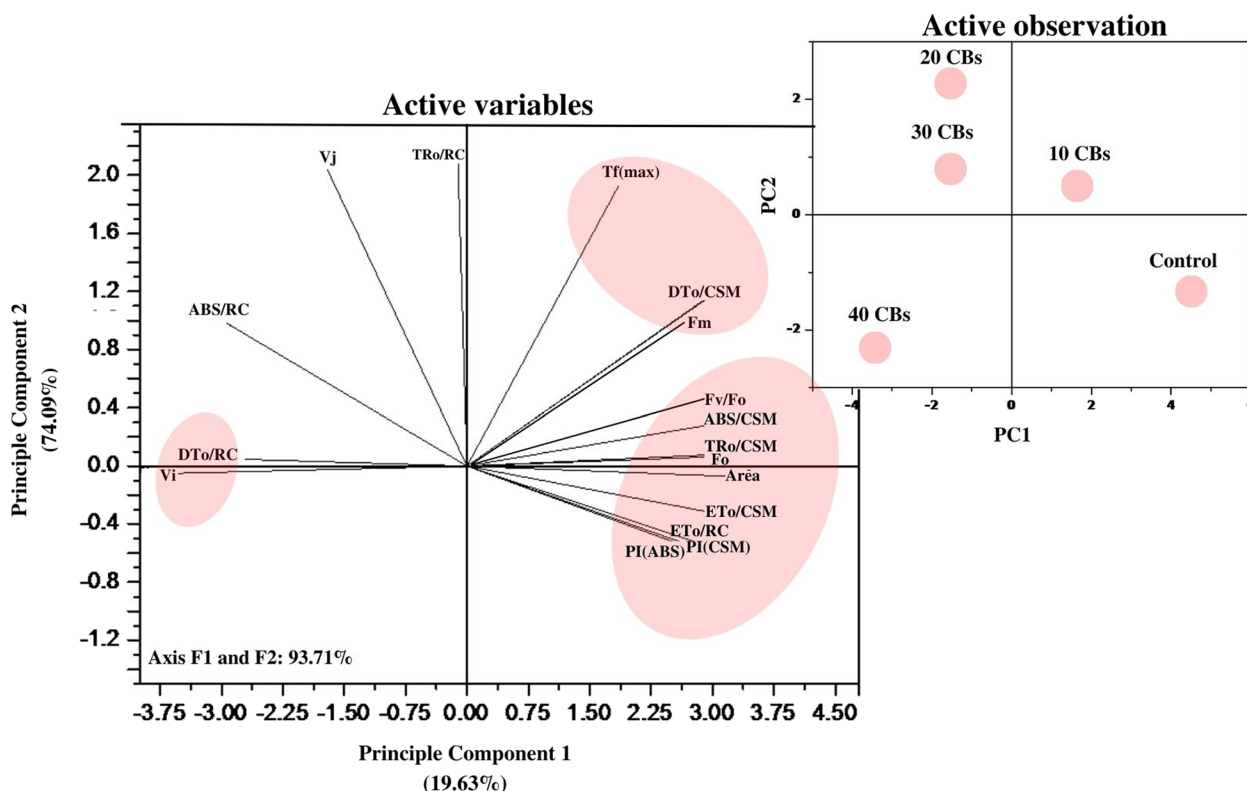


Fig. 6 A Principal Component Analysis (PCA) was conducted using chlorophyll fluorescence data for four different CBs treatment conditions. The PCA generated two dimensions (PC1 and PC2), with PC2 capturing the majority of the variance in the data. The Chlorophyll a fluorescence parameter was represented by arrows on the PC1 and PC2 dimensions. All calculated chlorophyll a fluorescence parameters. The correlations were represented with a color code.

IV. However, the 40 CBs treatment has a longer loading arrow than others in all quadrants, indicating that it significantly affects the major JIP parameters located in quadrant I and III (Fig. 6). Along this correlation matrix has been showing for all parameters in Fig. 7.

The LD₅₀ and LD₉₀ values for *A. pinnata*, which were calculated by number of mortality rate through probit analysis with a 95 % probability level displays in Table 4. LD₅₀ and LD₉₀ represent the lethal dose necessary to cause 50 % and 90 % mortality, respectively. The values obtained for LD₅₀ is 20.30 CBs and LD₉₀ is 35.26 CBs.

Discussion

Numerous studies have investigated the physiological adaptations of plants subjected to various stresses, which have revealed that plants have developed intricate defense mechanisms to counteract the detrimental effects of these environmental stressors [45, 47, 48]. The technique of chlorophyll *a* fluorescence (ChlF) analysis has been widely employed to detect composite biochemical changes occurring in the photosynthetic apparatus of

plants, encompassing both terrestrial and aquatic species [49]. The present investigation focused on assessing the impact of CBs exposure on multiple fluorescence parameters of photosystem II in *Azolla pinnata*.

Morphological parameters

The toxicity of CBs is widely acknowledged to have an adverse impact on the growth and physiological health of aquatic plants, albeit the degree of impact may vary depending on the specific plant species. In this particular study, it was observed that exposure to low concentrations of CBs (10) resulted in a minor reduction in frond area and root length in *A. pinnata* plants. However, as the concentration of CBs increased (≥ 20 CBs), a significant reduction in frond area and root length was observed. Previous studies also demonstrate that lower concentration produces less effect where as high concentration greater than 20 Earlier results also retarded the plant growth [50]. The notable decline in AFA and ARL at higher CBs concentrations suggests a negative correlation between CBs and plant growth. Furthermore, over

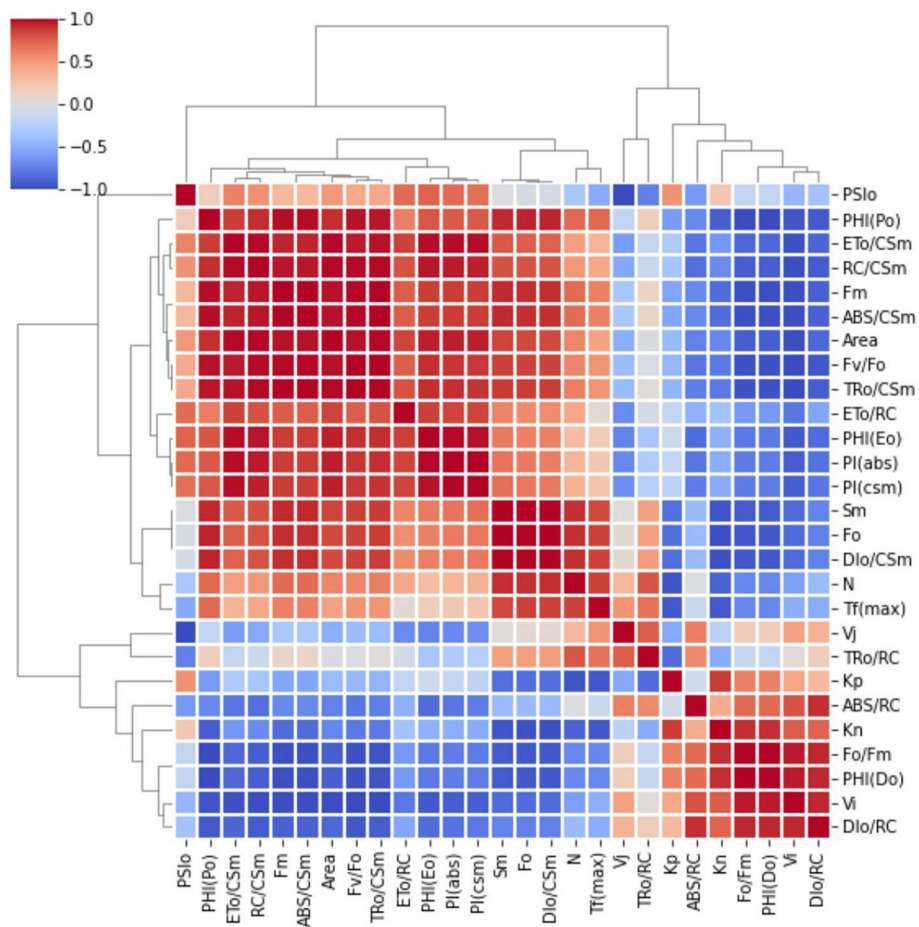


Fig. 7 Grid correlation matrix shows the correlation between all calculated chlorophyll *a* fluorescence parameter (with color code)

Table 4 The probit analysis was used to determine the acute 48-hour LD₅₀ values of CBs in *A. pinnata*, along with their corresponding confidence limits. The logarithm used in the analysis was base 10

	Confidence Limits						
	Probability	95% Confidence Limits for treatment			95% Confidence Limits for log(treatment) ^a		
		Estimate	Lower Bound	Upper Bound	Estimate	Lower Bound	Upper Bound
PROBIT	.010	7.453	5.243	9.347	.872	.720	.971
	.020	8.381	6.096	10.303	.923	.785	1.013
	.030	9.030	6.706	10.962	.956	.826	1.040
	.040	9.551	7.204	11.486	.980	.858	1.060
	.050	9.996	7.635	11.933	1.000	.883	1.077
	.060	10.392	8.022	12.328	1.017	.904	1.091
	.070	10.751	8.376	12.685	1.031	.923	1.103
	.080	11.084	8.706	13.015	1.045	.940	1.114
	.090	11.395	9.018	13.323	1.057	.955	1.125
	.100	11.690	9.313	13.614	1.068	.969	1.134
	.150	12.992	10.638	14.897	1.114	1.027	1.173
	.200	14.129	11.813	16.016	1.150	1.072	1.205
	.250	15.184	12.912	17.059	1.181	1.111	1.232
	.300	16.199	13.974	18.069	1.209	1.145	1.257
	.350	17.199	15.020	19.078	1.236	1.177	1.281
	.400	18.205	16.068	20.109	1.260	1.206	1.303
	.450	19.235	17.131	21.185	1.284	1.234	1.326
	.500	20.305	18.220	22.331	1.308	1.261	1.349
	.550	21.434	19.348	23.576	1.331	1.287	1.372
	.600	22.647	20.530	24.956	1.355	1.312	1.397
	.650	23.972	21.786	26.518	1.380	1.338	1.424
	.700	25.452	23.145	28.327	1.406	1.364	1.452
	.750	27.152	24.653	30.485	1.434	1.392	1.484
	.800	29.179	26.388	33.158	1.465	1.421	1.521
	.850	31.734	28.495	36.661	1.502	1.455	1.564
	.900	35.269	31.300	41.713	1.547	1.496	1.620
	.910	36.180	32.007	43.049	1.558	1.505	1.634
	.920	37.197	32.789	44.555	1.571	1.516	1.649
	.930	38.347	33.666	46.278	1.584	1.527	1.665
	.940	39.675	34.668	48.289	1.599	1.540	1.684
	.950	41.245	35.841	50.698	1.615	1.554	1.705
	.960	43.169	37.262	53.693	1.635	1.571	1.730
	.970	45.658	39.076	57.634	1.660	1.592	1.761
	.980	49.190	41.610	63.347	1.692	1.619	1.802
	.990	55.320	45.912	73.572	1.743	1.662	1.867

^a Logarithm base = 10

time, plant mortality rates increased with CBs treatment, and a decrease in frond number was attributed to excessive exposure to CBs, which also negatively impacted survival.

Biophysical parameters

The minimal fluorescence intensity values serve as a crucial parameter that can offer valuable information on the

irreparable harm caused to PSII, which is connected to the light-harvesting complex II (LHCII), this damage can impede the transfer of e⁻ on the reduced side of PSII [51, 52]. A decrease in minimal fluorescence under high CBs stress could be associated with less efficient PSII activity due to conformational changes in the D1 protein caused by CBs stress, which further result in alterations in the properties of PSII electron acceptors [51].

The F_V/F_0 parameter is utilized to determine the highest achievable 1° yield of photochemistry by considering concurrent variations in F_M and F_0 . When fronds are exposed to CBs stress, there is a decrease in F_V/F_0 values, which signifies alterations in the electron transport rate to the 1° electron acceptors from PSII and a reduction in the quantity and size of the reaction center. Previous studies have also documented a decrease in the F_V/F_0 ratio in different plant species due to environmental stress [53, 54]. The elevated level of relative variable fluorescence (V_j) under CBs treatment suggests that the electron transfer at the donor side of PSII has been affected. The modified unquenchable fluorescence (F_0) may have disrupted the energy transfer from the antenna complex to the reaction center, which in turn can impact F_V/F_0 . The PCA analysis reveals a positive correlation between the dissipation per reaction center (DT_0/RC) and the relative variable fluorescence V_j , whereas a negative correlation is observed with F_0 . This correlation is further validated by the correlation matrix (Fig. 7).

The analysis of fluorescence transients, also known as the "JIP test," in photosynthetic organisms subjected to abiotic stress has indicated a significant decline in the value of ϕP_0 [55]. This decrease in ϕP_0 can be attributed to a reduction in the photochemical efficiency of PSII caused by CBs-induced stress. Specifically, under light conditions, the reduction in the maximum quantum yield of PSII (ϕP_0) signifies that CBs stress impedes the redox reaction following Q_A and delays electron transport between Q_A^- and Q_B [56]. These parameters are crucial for gaining insights into the electron transport activity at the PSII acceptor sites. The findings of the present study suggest that CBs treatment leads to a reduction in electron transport at the PSII acceptor site in *A. pinnata* [57].

The energy pipeline models, such as the membrane and leaf model presented in Fig. 5(I) & (II), have demonstrated that several sites in PSII are sensitive to multiple environmental strain [58, 59]. The results of the present study indicate that the efficiency of trapping of electron and transport of electron from PSII decreases with an increasing concentration of CBs, as active RC is converted into inactive RC (denoted as dark circle in model). This is reflected in the decrease of TR_0/CSm and ET_0/CSm values [39, 41, 60]. The ABS/RC ratio is resolute by the total amount of photons captured by Chl molecules all over RC, divided by the total number of active RC [61]. The ratio of active to inactive RC affects this value, with an increase in active RC resulting in an increased ABS/RC ratio. The TR_0/RC ratio is an indicator of the maximal rate at which an exciton is captured by the RC, resulting in a decrease in the population of the 1° electron acceptor (Q_A). An increase in this ratio implies a reduction in the amount of Q_A that remains reduced. The decrease

in the ET_0/RC ratio signifies a reduced capacity for electron transport in inactive RC to re-oxidize the reduced Q_A , as more active RC is available. The total dissipation of un-trapped excitation energy from all RC, divided by the number of active RC, gives the DI_0/RC ratio, which is influenced by the ratios of active to inactive RC. The dissipation can take place via several pathways, including heat, fluorescence, and energy transfer to other systems and the ratio of active to inactive RC affects this dissipation. However, despite the impact of active/inactive RC ratios, the DI_0/RC ratio is not significantly affected due to the efficient use of energy by active RC [62, 63].

The F_V/F_M ratio is a crucial parameter in the JIP test that reflects the efficiency of 1° light energy conversion in the PSII reaction center. It serves as a stress indicator in many photosynthetic studies [55, 56, 64, 65]. However, this ratio is reliant on the fluorescence levels of F_0 and F_M , and any decrease in F_M value can result in a reduction in F_V/F_M ratio with increasing CBs. A novel and more responsive parameter called the Performance Index for measuring photosynthetic efficiency under stress [65, 66]. The performance index is derived from three or four components based on the density of reaction centers, trapping efficiency, and electron transport efficiency, much like the Goldman equation [67]. Food and productivity of plants are highly sensible with the entrapment of electron through the light reaction. Photosynthesis performance enroll the capability in plant to produce energy for growth and development [68, 69].

The performance index of a plant is a sensitive measure of the effects of stress on its components. Performance index is calculated based on energy absorption (PI_{ABS}) and cross-section (PI_{CS}), with the latter being dependent on the phenomenological energy flux. Our study found that the presence of CBs significantly lowered the values of PI_{ABS} and PI_{CS} in *A. pinnata*. This decrease in PI_{ABS} was attributed to reduced activity of the RC, which ultimately decreased the overall activity of the RC [30, 51, 70]. Using statistical models such as PCA and Correlation matrix, we identified several JIP parameters, including ABS/CSm , TR_0/CSm , ET_0/CSm , ϕP_0 , PI_{ABS} and PI_{CS} , which exhibited a dose-response relationship under CBs stress. Furthermore, the LD_{50} values of CBs, obtained through probit analysis, indicated that this molecule is highly toxic to *A. pinnata*.

Limitation and future aspects

Cigarette litter, particularly the disposal of CBs, is often driven by misconceptions regarding their environmental impact and perceived rapid biodegradability. A significant proportion of smokers, such as 43% surveyed in Germany [35, 71], are unaware that cigarette filters are predominantly composed of synthetic material,

specifically cellulose acetate—a type of plastic. Despite this composition, CBs are not widely recognized as single-use plastics. However, emerging evidence from various studies has demonstrated the detrimental effects of CBs on terrestrial, freshwater, and marine ecosystems [2, 7, 21]. The prolonged presence of these filters can have adverse ecological consequences, including diminished growth and biomass of economically significant primary producers, potentially leading to cascading effects on entire ecosystems.

As a result, there is an urgent need to reclassify cellulose acetate CBs globally as single-use plastics. Such a classification is crucial to improve regulations pertaining to their usage, collection, and disposal. To safeguard the environment effectively, a multifaceted approach is required. This includes raising awareness through targeted campaigns that educate the public about the severe impacts of cigarette litter. Furthermore, imposing higher fines and implementing smoking bans in ecologically sensitive areas [72] can act as deterrents. Additionally, extended producer responsibility must be enforced on tobacco companies, compelling them to take accountability for the collection, transportation, processing, and disposal of tobacco product waste. It is evident from interviews conducted by [73] that smokers often do not perceive cigarette filters as litter, highlighting the necessity of fostering public awareness regarding the long-lasting persistence of even biodegradable filters in the environment [74].

Conclusions

In conclusion, the current study provides compelling evidence of the significant impact of CBs on the morphology, ChlF kinetics and photosynthesis efficiency of *A. pinnata* plants, primarily by modulating the photosynthetic process. The study indicates that the introduction of CBs led to a decrease in chlorophyll fluorescence kinetics, quantum yield, and energy fluxes related to electron transport, while the energy fluxes related to absorption and dissipation increased. These findings suggest that CBs interfere with the photosynthetic process and alter the functioning of the PSII reaction centers, resulting in reduced growth and productivity of *A. pinnata*. The study highlights the need to regulate the use of CBs to mitigate their potential impact on plant growth and productivity. On the basis of lethal dose value (LD₅₀ and LD₉₀) plants are not able to survive on average 20–30 CBs concentration. Raising awareness regarding the long-lasting effects of cigarette filters, despite their biodegradability, is essential. Such CBs may persist in the environment for extended periods, leading to detrimental ecological consequences. They can curtail the growth and biomass of primary producers with economic significance,

resulting in cascading impacts on ecosystems. There is a paucity of knowledge about the negative impacts of discarded CBs on terrestrial and aquatic ecosystems. Thus, it is imperative to acknowledge this concern and take appropriate measures to alleviate the harmful influence of CBs on the environment.

Ethics approval and consent to participate

I declare that experimental research and field studies on plants (either cultivated or wild), must comply with the relevant institutional, national, and international guidelines of OECD 2002 and legislation. All methods were performed in accordance with the relevant guidelines and regulations.

Consent for publication

Not applicable.

Competing interests

The author declare that they have no competing financial interest or personal relationship that

Abbreviations

CBs	Cigarette butts
RC	Reaction center
PSI	Photosystem I
PSII	Photosystem II
ChlF	Chlorophyll <i>a</i> fluorescence

Acknowledgments

Author would like to acknowledge Mohanlal Sukhadia University, Udaipur for providing lab facilities.

Consent to participate

Not applicable.

Authors' contributions

VS and RJS conceived the idea, GS worked on experimental design and and GS wrote the whole manuscript. HS, JS and DK create graphs and statistical analysis. UB revised and edited complete manuscript. The complete manuscript was supervised and revised by VS.

Funding

This research did not receive any specific grant from funding agencies in the public, commercial, or not-for-profit sectors could have appear to influence the work reported in this paper.

Availability of data and materials

The data and materials that support the findings of the study are available from the corresponding author upon request.

Declarations

Consent for publication

Not applicable.

Competing interests

The authors declare no competing interests.

Received: 8 April 2023 Accepted: 5 April 2024
Published: 18 April 2024

References

- Conservancy O. International coastal cleanup report. 2019.
- Araújo MCB, Costa MF. A critical review of the issue of cigarette butt pollution in coastal environments. *Environ Res.* 2019;172:137–49.
- Patel V, Thomson GW, Wilson N. Cigarette butt littering in city streets: a new methodology for studying and results. *Tob Control.* 2013;22:59–62.
- Moriwaki H, Kitajima S, Katahira K. Waste on the roadside, 'poi-sute'waste: its distribution and elution potential of pollutants into environment. *Waste Manag.* 2009;29:1192–7.
- Schneider JE, Scheibling CM, Peterson NA, Stigler Granados P, Fulton L, Novotny TE. Online simulation model to estimate the total costs of tobacco product waste in large US cities. *Int J Environ Res Public Health.* 2020;17:4705.
- Wilson N, Oliver J, Thomson G. Smoking close to others and butt littering at bus stops: pilot observational study. *PeerJ.* 2014;2:e272.
- Dobaradaran S, Schmidt TC, Lorenzo-Parodi N, Kazipur-Cegla W, Jochmann MA, Nabipour I, et al. Polycyclic aromatic hydrocarbons (PAHs) leachates from cigarette butts into water. *Environ Pollut.* 2020;259:113916.
- Green ALR, Putschew A, Nehls T. Littered cigarette butts as a source of nicotine in urban waters. *J Hydrol.* 2014;519:3466–74.
- Novotny TE, Hardin SN, Hovda LR, Novotny DJ, McLean MK, Khan S. Tobacco and cigarette butt consumption in humans and animals. *Tob Control.* 2011;20(Suppl 1):i17–20.
- Dobaradaran S, Schmidt TC, Kazipur-Cegla W, Jochmann MA. BTEX compounds leachates from cigarette butts into water environment: a primary study. *Environ Pollut.* 2021;269:116185.
- Dobaradaran S, Schmidt TC, Mutke XAM, De-la-Torre GE, Telgheder U, Kerpen K, et al. Aromatic amines leachate from cigarette butts into aquatic environments: Is there risk for water organisms? *Environ Res.* 2023;216:114717.
- Dobaradaran S, Nabipour I, Saeedi R, Ostovar A, Khorsand M, Khajeahmadi N, et al. Association of metals (Cd, Fe, As, Ni, Cu, Zn and Mn) with cigarette butts in northern part of the Persian Gulf. *Tob Control.* 2017;26:461–3.
- Slaughter E, Gersberg RM, Watanabe K, Rudolph J, Stransky C, Novotny TE. Toxicity of cigarette butts, and their chemical components, to marine and freshwater fish. *Tob Control.* 2011;20(Suppl 1):i25–9.
- Dobaradaran S, Soleimani F, Akhbarizadeh R, Schmidt TC, Marzban M, BasirianJahromi R. Environmental fate of cigarette butts and their toxicity in aquatic organisms: a comprehensive systematic review. *Environ Res.* 2021;195:110881.
- Matt GE, Quintana PJE, Destaillets H, Gundel LA, Sleiman M, Singer BC, et al. Thirdhand tobacco smoke: emerging evidence and arguments for a multidisciplinary research agenda. *Environ Health Perspect.* 2011;119:1218–26.
- Hoffmann DHI. The changing cigarette, 1950–1995. *J Toxicol Environ Health Part A.* 1997;50(4):307–64.
- Patel M, Cuccia AF, Folger S, Benson AF, Vallone D, Novotny TE. Support for cigarette filter waste policies among US adults. *Tob Control.* 2021.
- Micevska T, Warne MSJ, Pablo F, Patra R. Variation in, and causes of, toxicity of cigarette butts to a cladoceran and microtox. *Arch Environ Contam Toxicol.* 2006;50:205–12.
- Wright SL, Rowe D, Reid MJ, Thomas KV, Galloway TS. Bioaccumulation and biological effects of cigarette litter in marine worms. *Sci Rep.* 2015;5:1–10.
- Booth DJ, Gribben P, Parkinson K. Impact of cigarette butt leachate on tidepool snails. *Mar Pollut Bull.* 2015;95:362–4.
- Soleimani F, Dobaradaran S, Mohebbi G, Vazirizadeh A, De-la-Torre GE, Saeedi R, et al. Toxic effect of cigarette butts leachates on blood markers of *Periophthalmus waltoni* species from the Persian Gulf region. *Chemosphere.* 2023;319:138036.
- Selmar D, Radwan A, Abdalla N, Taha H, Wittke C, El-Henawy A, et al. Uptake of nicotine from discarded cigarette butts—A so far unconsidered path of contamination of plant-derived commodities. *Environ Pollut.* 2018;238:972–6.
- Montalvão MF, Sampaio LLG, Gomes HHH, Malafai G. An insight into the cytotoxicity, genotoxicity, and mutagenicity of smoked cigarette butt leachate by using *Allium cepa* as test system. *Environ Sci Pollut Res.* 2019;26:2013–21.
- Akhbarizadeh R, Dobaradaran S, Parhizgar G, Schmidt TC, Mallaki R. Potentially toxic elements leachates from cigarette butts into different types of water: a threat for aquatic environments and ecosystems? *Environ Res.* 2021;202:111706.
- Miranda AF, Kumar NR, Spangenberg G, Subudhi S, Lal B, Mouradov A. Aquatic plants, *Landoltia punctata*, and *Azolla filiculoides* as bioconverters of wastewater to biofuel. *Plants.* 2020;9:437.
- Elrasoul ASA, Mousa AA, Orabi SH, Mohamed MAEG, Gad-Allah SM, Almeer R, et al. Antioxidant, anti-inflammatory, and anti-apoptotic effects of *Azolla pinnata* ethanolic extract against lead-induced hepatotoxicity in rats. *Antioxidants.* 2020;9:1014.
- Sarkar A, Jana S. Heavy metal pollutant tolerance of *Azolla pinnata*. *Water Air Soil Pollut.* 1986;27:15–8.
- Kooh MRR, Lim LBL, Lim LH, Dahri MK. Separation of toxic rhodamine B from aqueous solution using an efficient low-cost material, *Azolla pinnata*, by adsorption method. *Environ Monit Assess.* 2016;188:1–15.
- Percival GC, Keary IP, Sulaiman A-H. An assessment of the drought tolerance of *Fraxinus* genotypes for urban landscape plantings. *Urban For Urban Green.* 2006;5:17–27.
- Kumar D, Singh H, Raj S, Soni V. Chlorophyll a fluorescence kinetics of mung bean (*Vigna radiata* L.) grown under artificial continuous light. *Biochem Biophys Reports.* 2020;24:100813.
- Ashraf S, Ali Q, Zahir ZA, Ashraf S, Asghar HN. Phytoremediation: Environmentally sustainable way for reclamation of heavy metal polluted soils. *Ecotoxicol Environ Saf.* 2019;174:714–27.
- Yadav SK. Heavy metals toxicity in plants: an overview on the role of glutathione and phytochelatin in heavy metal stress tolerance of plants. *South African J Bot.* 2010;76:167–79.
- Soleimani F, Dobaradaran S, De-la-Torre GE, Schmidt TC, Saeedi R. Content of toxic components of cigarette, cigarette smoke vs cigarette butts: a comprehensive systematic review. *Sci Total Environ.* 2022;813:152667.
- Shah G, Bhatt U, Soni V. Cigarette: an unsung anthropogenic evil in the environment. *Environ Sci Pollut Res.* 2023;30(21):59151–62.
- Green DS, Boots B, Carvalho JDS, Starkey T. Cigarette butts have adverse effects on initial growth of perennial ryegrass (gramineae: *Lolium perenne* L.) and white clover (leguminosae: *Trifolium repens* L.). *Ecotoxicol Environ Saf.* 2019;182:109418.
- Zazouli MA, Mahdavi Y, Bazrafshan E, Balarak D. Phytodegradation potential of bisphenol A from aqueous solution by *Azolla filiculoides*. *J Environ Heal Sci Eng.* 2014;12:1–5.
- Strasser R. On the OJIP fluorescence transient in leaves and D1 mutants of *Chlamydomonas reinhardtii*. In: Research in photosynthesis: proceedings of the IXth International Congress on Photosynthesis. Vol. 2. Kluwer Academic Publishers; 1992. p. 29–32.
- Strasser RJ, Srivastava A, Tsimilli-Michael M. The fluorescence transient as a tool to characterize and screen photosynthetic samples. *Probing Photosynth Mech Regul Adapt.* 2000;25:445–83.
- Tsimilli-Michael M. Revisiting JIP-test: An educative review on concepts, assumptions, approximations, definitions and terminology. *Photosynthetica.* 2020;58:275–92.
- Stirbet A. On the relation between the Kautsky effect (chlorophyll a fluorescence induction) and photosystem II: basics and applications of the OJIP fluorescence transient. *J Photochem Photobiol B Biol.* 2011;104:236–57.
- Strasser RJ, Srivastava A. Polyphasic chlorophyll a fluorescence transient in plants and cyanobacteria. *Photochem Photobiol.* 1995;61:32–42.
- Gomez-Flores A, Bradford SA, Cai L, Urik M, Kim H. Prediction of attachment efficiency using machine learning on a comprehensive database and its validation. *Water Res.* 2023;229:119429.
- Sangani MF, Owens G, Nazari B, Astaraei A, Fotovat A, Emami H. Different modelling approaches for predicting titanium dioxide nanoparticles mobility in intact soil media. *Sci Total Environ.* 2019;665:1168–81.
- Bhatt U, Singh H, Kumar D, Soni V. Rehydration quickly assembles photosynthetic complexes in desiccation tolerant *Riccia gangetica*. *Biomed J Sci Tech Res.* 2020;30:23034–7.

45. Bhatt U, Singh H, Kumar D, Soni V. Rehydration induces quick recovery of photosynthesis in desiccation tolerant moss *Semibarbula orientalis*. *J Plant Sci Res*. 2019;35:183–7.
46. Bhatt U, Singh H, Kumar D, Strasser RJ, Soni V. Severe leaf-vein infestation upregulates antioxidant and photosynthetic activities in the lamina of *Ficus religiosa*. *Acta Physiol Plant*. 2022;44:15.
47. Sharma S, Bhatt U, Sharma J, Darkalt A, Mojski J, Soni V. Effect of different waterlogging periods on biochemistry, growth, and chlorophyll a fluorescence of *Arachis hypogaea* L. *Front Plant Sci*. 2022;13:1006258.
48. Sharma J, Singh H, Sharma S, Kumar D, Bhatt U, Soni V. Rhodamine B induced alteration in antioxidant enzymes and photosynthetic performance of *Eichhornia crassipes*. *Plant Physiol Rep*. 2022;27:603–17.
49. Gonzalez-Mendoza D, Escoboza-García F, Santamaría JM, Zapata-Perez O. Copper stress on photosynthesis of black mangle (*Avicennia germinans*). *An Acad Bras Cienc*. 2013;85:665–70.
50. Prasad SM, Singh A, Singh P. Physiological, biochemical and growth responses of *Azolla pinnata* to chlorpyrifos and cypermethrin pesticides exposure: a comparative study. *Chem Ecol*. 2015;31:285–98.
51. Kalaji HM, Schansker G, Ladle RJ, Goltsev V, Bosa K, Allakhverdiev SI, et al. Frequently asked questions about in vivo chlorophyll fluorescence: practical issues. *Photosynth Res*. 2014;122:121–58.
52. Goltsev VN, Kalaji HM, Paunov M, Bąba W, Horaczek T, Mojski J, et al. Variable chlorophyll fluorescence and its use for assessing physiological condition of plant photosynthetic apparatus. *Russ J Plant Physiol*. 2016;63:869–93.
53. Martinazzo EG, Ramm A, Bacarin MA. The chlorophyll a fluorescence as an indicator of the temperature stress in the leaves of *Prunus persica*. *Brazilian J Plant Physiol*. 2012;24:237–46.
54. Janka E, Körner O, Rosenqvist E, Ottosen C-O. High temperature stress monitoring and detection using chlorophyll a fluorescence and infrared thermography in chrysanthemum (*Dendranthema grandiflora*). *Plant Physiol Biochem*. 2013;67:87–94.
55. Baker AJM, Brooks R. Terrestrial higher plants which hyperaccumulate metallic elements. A review of their distribution, ecology and phytochemistry. *Biorecovery*. 1989;1:81–126.
56. Schansker G, Tóth SZ, Strasser RJ. Methylviologen and dibromothymoquinone treatments of pea leaves reveal the role of photosystem I in the Chl a fluorescence rise OJIP. *Biochim Biophys Acta (BBA)-Bioenergetics*. 2005;1706:250–61.
57. Mykhaylenko NF, Zolotareva EK. The effect of copper and selenium nanocarboxylates on biomass accumulation and photosynthetic energy transduction efficiency of the green algae *Chlorella vulgaris*. *Nanoscale Res Lett*. 2017;12:147.
58. Zushi K, Kajiwara S, Matsuzoe N. Chlorophyll a fluorescence OJIP transient as a tool to characterize and evaluate response to heat and chilling stress in tomato leaf and fruit. *Sci Hortic (Amsterdam)*. 2012;148:39–46.
59. Gautam A, Agrawal D, SaiPrasad SV, Jajoo A. A quick method to screen high and low yielding wheat cultivars exposed to high temperature. *Physiol Mol Biol Plants*. 2014;20:533–7.
60. Zushi K, Matsuzoe N. Using of chlorophyll a fluorescence OJIP transients for sensing salt stress in the leaves and fruits of tomato. *Sci Hortic (Amsterdam)*. 2017;219:216–21.
61. Rapacz M, Sasal M, Kalaji HM, Kościelniak J. Is the OJIP test a reliable indicator of winter hardiness and freezing tolerance of common wheat and triticale under variable winter environments? *PLoS One*. 2015;10:e0134820.
62. Grieco M, Suorsa M, Jajoo A, Tikkanen M, Aro E-M. Light-harvesting II antenna trimers connect energetically the entire photosynthetic machinery—including both photosystems II and I. *Biochim Biophys Acta (BBA)-Bioenergetics*. 2015;1847:607–19.
63. Heber U, Soni V, Strasser RJ. Photoprotection of reaction centers: thermal dissipation of absorbed light energy vs charge separation in lichens. *Physiol Plant*. 2011;142:65–78.
64. Kalaji HM, Goltsev V, Bosa K, Allakhverdiev SI, Strasser RJ. Experimental in vivo measurements of light emission in plants: a perspective dedicated to David Walker. *Photosynth Res*. 2012;114:69–96.
65. Baker RR, da Silva JRP, Smith G. The effect of tobacco ingredients on smoke chemistry. Part I: Flavourings and additives. *Food Chem Toxicol*. 2004;42:3–37.
66. Srivastava A, Strasser RJ. Greening of peas: parallel measurements of 77 K emission spectra, OJIP chlorophyll a fluorescence transient, period four oscillation of the initial fluorescence level, delayed light emission, and P700. *Photosynthetica*. 1999;37:365–92.
67. Goldman DE. Potential, impedance, and rectification in membranes. *J Gen Physiol*. 1943;27:37–60.
68. Sharma J, Shah G, Strasser RJ, Soni V. Effects of malachite green on biochemistry and photosystem II photochemistry of *Eichhornia crassipes*. *Funct Plant Biol*. 2023;50:663–75.
69. Zhang J, Zhang H, Srivastava AK, Pan Y, Bai J, Fang J, et al. Knockdown of rice microRNA166 confers drought resistance by causing leaf rolling and altering stem xylem development. *Plant Physiol*. 2018;176:2082–94.
70. Kalaji HM, Schansker G, Brestic M, Bussotti F, Calatayud A, Ferroni L, et al. Frequently asked questions about chlorophyll fluorescence, the sequel. *Photosynth Res*. 2017;132:13–66.
71. Kotz D, Kastaun S. Do people know that cigarette filters are mainly composed of synthetic material? A representative survey of the German population (the DEBRA study). *Tob Control*. 2021;30:345–7.
72. Axelsson C, van Sebille E. Prevention through policy: Urban macroplastic leakages to the marine environment during extreme rainfall events. *Mar Pollut Bull*. 2017;124:211–27.
73. Rath JM, Rubenstein RA, Curry LE, Shank SE, Cartwright JC. Cigarette litter: smokers' attitudes and behaviors. *Int J Environ Res Public Health*. 2012;9:2189–203.
74. Shah G, Bhatt U, Soni V (2023). A comprehensive review on triple R eco-management strategies to reduce, reuse and recycle of hazardous cigarette butts. *Heliyon*.

Publisher's Note

Springer Nature remains neutral with regard to jurisdictional claims in published maps and institutional affiliations.